Error Events Due to Island Size Variations in Bit Patterned Media

Yuanjing Shi, Paul W. Nutter, Branson D. Belle, and Jim J. Miles

Nano Engineering & Storage Technology Research Group, School Of Computer Science, The University of Manchester, Manchester, M13 9PL, UK

Control of the variations of island properties is one of the key challenges in fabricating Bit-Patterned Media for future storage systems. The presence on any variation in the size and position of an island has a detrimental effect on the ability to recover recorded data, particularly in the case of variation in island size. By analyzing error events when island size variations are present we have identified that these are more likely to be single-bit in nature. To understand the origins of these error events we have investigated the size and magnetization state of islands in the vicinity where a single-bit error event is encountered. It is shown that these error events occur due to particular combinations of island size and magnetization state for the three islands investigated. In every case the central island, from which the data bit is recovered in error, is small compared to the nominal island size. These results show that size variations must be controlled in the fabrication process in order to maximize the bit-error-rate performance of the read channel.

***Index Terms*—Bit patterned media, error events, magnetic recording, position variations, read channel, size variations.**

I. Introduction

THE INCREASING demand for higher storage capacities in magnetic disc drives requires a storage density in excess of 1 Tb/in^2. It is generally recognised that bit-patterned media (BPM) using perpendicular recording may be a future solution that will permit ultrahigh areal densities in excess of 1 Tbit/in^2 [1], [2]. In BPM, each information bit is recorded to a patterned, isolated, single-domain magnetic island. One of the problems associated with the fabrication of island arrays for BPM is the variability of island position and island size, both of which have a detrimental effect on the writing and reading of information [3]–[5]. Since variations of island geometry due to imperfect fabrication are unavoidable, the understanding of the effect of such variations upon bit-error-rate (BER) performance is a primary challenge in BPM [2], [5]. The effect of island position, or location, variations on the recovery of recorded data has been studied in [4]. In practical media the use of electron beam lithography or self-assembly techniques often produce island arrays of regular island position, i.e., controlled period, but there may still be a severe variation in the island size [6], and the impact of size variations upon BER performance is therefore important [7].

In conventional magnetic recording the size and bit-aspect-ratio (BAR) of the recorded magnetic domains are determined by the dimensions of the recording head, whereas in BPM the fabrication process itself determines these properties. Most approaches to fabricating BPM result in a BAR of 1, i.e., the islands are of equal size along-track and across-track. However, a large BAR is desirable when using modern read/write heads due to a number of reasons: the ease of head fabrication, to improve write head fields, and to obtain acceptable replay waveform signal to noise ratio (SNR) [2]. Reference [5] lists a number of design scenarios for BPM at areal densities in the range of 1–5 Tbit/in^2, with many of the preferred designs having a BAR greater than 1. However, at any given density, raising the BAR above 1 will decrease one of the dimensions (typically the length along track) of the island, potentially resulting in broader distributions of the island properties, such as island period, island size and magnetic anisotropy [2], which may have an even greater effect on the BER performance of the read channel.

In this paper, the effect of island size variations on the raw BER performance in BPM systems with an island BAR of 4 is explored. We present an analysis of the resulting error events in order to understand the root causes of such errors, with respect to the island size variations and magnetization state. In this analysis the presence of other sources of error, such as inter-track interference (ITI) and additive white Gaussian noise (AWGN) have been removed.

II. Read Channel Model

A comprehensive read channel simulation has been developed that allows the investigation of the BER performance of a BPM storage system and, more importantly for the following analysis, allows error events to be identified. The read channel simulation employs a 3-D reciprocity replay model to generate replay signals arising from a large number of islands for a given giant magneto-resistive (GMR) read head design and BPM media design [8]. The replay model allows any variations in island geometry to be easily investigated. Generated replay signal samples are then analysed by a conventional partial-response maximum-likelihood (PRML) read channel, using a Viterbi decoder, to determine recorded data recovered in error.

In the following analysis, single-domain islands of nominal size along-track of 7.5 nm, period along-track of 15 nm with a $\mathrm{BAR} = 4$ (nominal width across-track of 30 nm and track pitch of 40 nm) are assumed, which supports an areal density of 1 Tb/in^2. The GMR read head adopted has sensor dimensions: width across-track of 20 nm, length along-track of 4 nm and shield-to-shield spacing of 16 nm [9]. The write process and the thermal stability of stored data are not considered in this paper, and so the magnetic properties of the islands have not been defined. Here we only concentrate on investigating the effect that variations in the position and size of islands have on the raw BER performance of the read channel. The effects of equalization and AWGN have not been included in order to isolate the effects of island geometry variations only. In addition, ITI has also been ignored since the island width across-track is larger

Manuscript received October 30, 2009; revised December 10, 2009; accepted January 12, 2010. Current version published May 19, 2010. Corresponding author: P. W. Nutter (e-mail: p.nutter@manchester.ac.uk).

Color versions of one or more of the figures in this paper are available online at http://ieeexplore.ieee.org.

Digital Object Identifier 10.1109/TMAG.2010.2041047

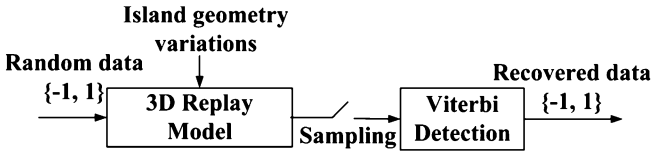

Fig. 1. Block diagram of the read channel model with island geometry variations.

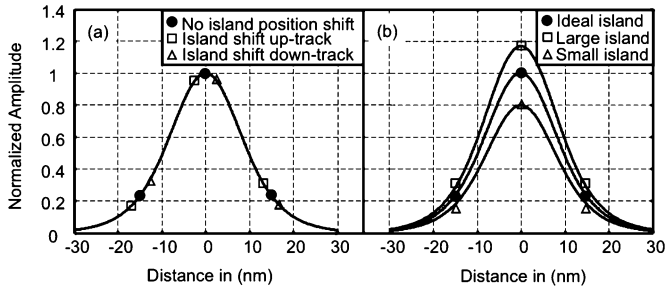

Fig. 2. Effects of (a) island position variations and (b) island size variations on the replay pulse sample values for an isolated island.

than the width of the GMR sensor. Fig. 1 illustrates a block diagram of the read channel model developed, where a generalized partial response (GPR) target of [0.25 1 0.25] is chosen to match the shape of the isolated (ideal) island response.

The replay waveform is produced by the superposition of island edge responses at positions defined by each island along the track. From these waveforms sample values are extracted corresponding to the (ideal) position of each island, i.e., at the ideal island period [4]. For example, Fig. 2 illustrates pulse responses generated by the superposition of leading and lagging edge responses. Variations of island position or size are introduced by varying the position at which these edge responses are superposed. In the case of variation in island position, the nominal position of each island is varied by shifting both edges of the island in the same direction (down-track or up-track). In the case of variations in island size an equal shift is applied to each edge of the island, but in opposite directions. Simultaneous position and size variations are generated by randomly shifting the edges of each island. These variations are assumed to be random with a truncated Gaussian distribution, of mean zero and standard deviation σ specified in nm, with the edge shift restricted so that there is no island overlap.

Let Δ_p denote the position shift of the island, then the replay pulse due the position shift can be represented by $h(x-\Delta_p)$, where $h(x)$ denotes the replay pulse due to an ideal island. Differences between the replay pulse and the position-shifted pulse can be expressed approximately as

$$\Delta h(x) = h(x) - h(x-\Delta_p) = \Delta_p \frac{dh(x)}{dx}. \qquad (1)$$

It can be seen from (1) that the effect of the position shift on the replay samples is related to the local slope of the replay pulse.

Fig. 2 illustrates the effect that an arbitrary amount of island position variation (Fig. 2(a)) and island size variation (Fig. 2(b)) will have on the replay samples due to an isolated island. Here the sample values, shown as the symbols on the curves of Fig. 2, have been taken at points corresponding to the ideal sampling time (in terms of distance from the island centre) of an island, plus an island pitch before and after the island of interest. In both Fig. 2(a) and (b) the circles indicate the ideal replay sample values with no variation in the island geometry. It can be seen from Fig. 2(a) that when island position shift is introduced, the central sample, corresponding to the sample at the centre of an island, is at, or close to, the peak of the pulse where the slope is near zero, and so there is a small effect on the sample value. At the samples either side of the central sample, which correspond to the ideal positions of adjacent islands, the pulse slope is larger and this will result in a variation in the amount of ISI in the waveform observed. Fig. 2(b) shows that island size variations have an impact on the magnitude of the sample value corresponding to the island of interest. An increase in the island size results in an increase in the signal magnitude and a decrease in the island size results in a decrease in the signal magnitude. These signal amplitude changes are expected since the replay signal is proportional to the flux emanating from the islands and the total amount of magnetic material present. In the case of the adjacent samples, little change in sample magnitude is observed resulting in a small change in the amount of ISI present. The effect of the two different variations of the island geometry (position and size) on the sample values may enable them to be distinguished on an island-by-island basis, which could be put to use in an advanced detector.

The effects of island position variations, island size variations, and both island position and size variations on the read channel performance in a high BAR system have been explored. Fig. 3 illustrates the BER performance versus the standard deviation, σ nm, of the island variations with no other sources of noise present. In the case of just island position variations (not shown) then no errors are detected. In the presence of just size variations then the number of errors increases with σ. In the case of the presence of both position and size variations (dashed line), where each has a standard deviation of $\sqrt{2}\cdot\sigma/2$ giving a total contribution of σ, then significantly more bit errors are observed compared with the cases of position and size variations alone. The results shown in Fig. 3 demonstrate the need to investigate the origins of errors in BPM when island variations are present. Here, we begin this analysis by considering the identification of error events in the presence of size variations only.

III. Identification of Error Events

The analysis of error events is essential for the performance analysis of read channels [10]. An error event is defined as a distinct distance between the correct path and the estimated path in the maximum-likelihood (ML) Viterbi detector. In the trellis, the error event occurs when the correct path and the estimated path start to diverge at one state, and it ends when those two paths converge into another state. Fig. 4 shows an example of the error event in a trellis for the GPR target used. The Viterbi detector compares the read-back samples, y_k, with the path metric to decide the transition from one state to another. It chooses the transition path for which the path metric has the minimum squared distance from the replay samples. The correct path (solid line) that the Viterbi detector should take is S1-S1-S1-S1, but because of the presence of island geometry variations the replay samples vary from the ideal samples and the Viterbi detector takes the erroneous path S1-S3-S2-S1 (dashed line). An error event starts at magnetization state S1 and ends at S1, between these two states the path goes though

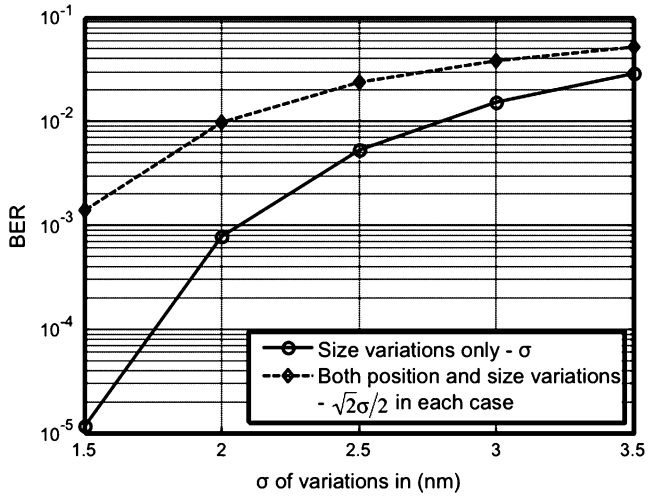

Fig. 3. BER curves for σ variation in island geometry for 1 Tb/in^2 BPM system.

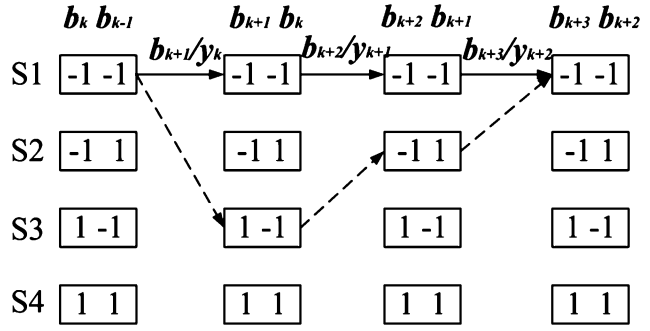

Fig. 4. Example of an error event in the trellis of Viterbi detector. The solid line shows the correct path and the dashed shows the erroneous path.

two incorrect states. The error event can also be represented by the associated input error sequence as $\varepsilon_b = b_k - d_k$, where $1 \leq k \leq l(\varepsilon), l(\varepsilon)$ is the length of an error event, $\varepsilon_b(k) = \{-2, 0, 2\}, b_k$ is the input data sequence to the PR channel, and d_k is the estimated recovered data sequence from the Viterbi detector. The number of bit errors due to an error event is equal to the number of non-zero coefficients in ε_b, which is represented as $\mathrm{w_H}(\varepsilon_b)$. It can be seen from the definition that the error event that extends from time $t_1 = k$ to $t_2 = k + 2$, will not have more than $v - 1$ consecutive zeros between time t_1 and $t_2 - v$, where v represents the memory in the channel (i.e., the length of the target minus one). While there are many possible error events in the read channel, a few typical error events may be the dominant source of errors. In order to identify the typical error events, the read channel simulation was run continuously to generate 4960×10^3 bits for the Viterbi detector to recover, from which the error sequences were identified and recorded. Here, the memory of the channel is 2.

If no more than two consecutive zeros are found in the error sequences between two non-zero values, then an error event is recognized. For example, a single bit error event can be indentified as "0 0 +2 0 0" and a two-bit error event can be indentified as "0 0 +2 −2 0 0" or "0 0 +2 0 −2 0 0." The distinct error events were searched in the results of the read channel simulation, with results shown in Table I, for island size (length along-track) standard deviations ranging from 1.5 nm to 3.5 nm (20% to 46% of

TABLE I
ERROR EVENT STATISTICS

$\mathrm{w_H}(\varepsilon_b)$	Standard Variation of Island Sizes (σ)				
	1.5nm	2.0nm	2.5nm	3.0nm	3.5nm
1 bit	100%	100%	99.69%	98.95%	97.92%
2 bits	0%	0%	0.31%	1.03%	1.96%
3 bits	0%	0%	0.005%	0.02%	0.09%

TABLE II
SIZE CHANGE STATISTICS FOR THE THREE ISLANDS OF INTEREST

Size Variation σ (nm)	Small Neighbors		Big Neighbors		Small Central Island	
	μ_d (nm)	σ_d (nm)	μ_d (nm)	σ_d (nm)	μ_d (nm)	σ_d (nm)
2.0	4.98	1.76	10.18	1.94	1.62	1.17
2.5	4.67	2.07	10.19	2.60	1.40	1.39
3.0	4.55	2.31	10.33	2.84	1.11	1.66
3.5	3.75	2.93	10.60	3.96	0.89	1.88

nominal island length). Table I shows that in all cases of σ investigated the dominant error events are single bit in nature, even as the standard deviation of the size variation is increased (over 95% of all the error events observed).

Once the error events have been identified the island properties (size and magnetization state) corresponding to the islands in the vicinity of each of the error events were investigated. For the GPR target chosen, three consecutive islands are considered that are centered on the island for which the magnetization state was recovered in error. The eight possible combinations of magnetization states for these three islands can be categorized into the four cases listed in the first column of Table II. In all cases the single bit error was only observed when the size of the centre island (the one recovered in error) was "small" compared to the nominal size of an island along track of 7.5 nm. In the case where the magnetization state of the neighboring islands differ from that of the centre island ($-,+,-$ or $+,-,+$) then an error event is more likely to be observed when they are 'big' compared with the nominal island size. Similarly, when the magnetization state of the neighboring islands is the same as that of the centre island ($-,-,-$ or $+,+,+$) then an error event is more likely to be observed when they are 'small' compared to the nominal size.

Fig. 5 illustrates distributions for the three islands identified, corresponding to the data bits recovered in error, when there are varying amount of island size variations present. Fig. 5 illustrates that in the error event cases observed the size distribution of the central island is a truncated Gaussian and that the size distributions for the neighboring islands (indicated as previous and next) correspond to two weighted Gaussian distributions arising from the "small" and "big" cases observed in Table II. Table III summarizes mean values (μ_d) and standard deviations (σ_d) for the distributions for the central islands and a combination of the distributions of the neighboring islands where an error event occurred, for each case of size variation (σ) investigated. In the case of the central island that is recovered in error, as the island size variation (σ) is increased then the mean value of the island distribution (μ_d) decreases, but the standard deviation (σ_d)

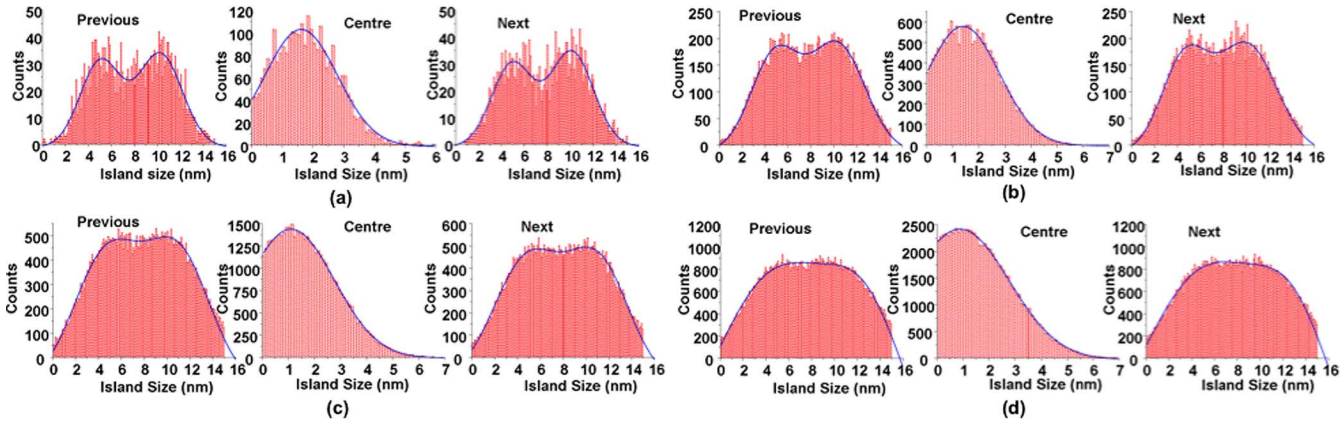

Fig. 5. Size distributions of the three islands of interest centred on the island corresponding to the data bit recovered in error. Four values of σ are considered: (a) 2.0 nm, (b) 2.5 nm, (c) 3 nm, (d) 3.5 nm (27% to 46% of nominal island length of 7.5 nm).

TABLE III
DISTRIBUTION STATISTICS FOR THE THREE ISLANDS OF INTEREST

Size Variation (nm)	Small Neighbors		Big Neighbors		Small Central Island	
	d (nm)	d (nm)	d (nm)	d (nm)	d (nm)	d (nm)
2.0	4.98	1.76	10.18	1.94	1.62	1.17
2.5	4.67	2.07	10.19	2.60	1.40	1.39
3.0	4.55	2.31	10.33	2.84	1.11	1.66
3.5	3.75	2.93	10.60	3.96	0.89	1.88

increases. In the case of the neighboring islands, a similar decrease in mean value is observed for the "small" islands, and an increase in mean value is observed for the "big" islands as the size variation increases. In both cases the standard deviation of the distributions increases as the size variation increases.

IV. CONCLUSION

In this paper, we have used a read channel simulation to show that fluctuations in the island size in BPM systems have a detrimental effect on the data recovery process, particularly in the case of high BAR islands. Here the analysis of errors shows that the dominant error events are single-bit in nature. Particular combinations of island size and magnetization state for a group of three islands are more likely to cause single-bit error events, more importantly when the central island is small (1.6 nm when $\sigma = 2$ nm, 0.9 nm when $\sigma = 3.5$ nm) in comparison with the nominal size of 7.5 nm. These results show that island size needs to be carefully controlled in the fabrication process in order to prevent single-bit errors from occurring, thus improving the BER performance. Alternatively, coding schemes should be adopted that mitigate the effects of such single-bit error events.

Future work will concentrate on determining BER performance using analytical approaches to enable a thorough investigation of the combined effects of position and size variations to understand the origins of the severe degradation in BER performance shown in Fig. 3.

ACKNOWLEDGMENT

This work was supported by the Engineering & Physical Sciences Research Council under Grant EP/E017657/1, and by the Information Storage Industry Consortium (INSIC) EHDR program.

REFERENCES

[1] H. J. Ritcher, "The transition from longitudinal to perpendicular recording," *J. Phys. D: Appl. Phys.*, vol. 40, pp. R149–R177, 2007.
[2] B. D. Terris, "Fabrication challenges for patterned recording media," *J. Magn. Magn. Mater.*, vol. 321, pp. 512–517, 2009.
[3] J. Kalezhi, J. J. Miles, and B. D. Belle, "Dependence of switching fields on island shape in bit patterned media," *IEEE Trans. Magn.*, vol. 45, no. 10, pp. 3531–3534, Oct. 2009.
[4] P. W. Nutter, Y. Shi, B. D. Belle, and J. J. Miles, "Understanding sources of errors in bit-patterned media to improve read channel performance," *IEEE Trans. Magn.*, vol. 44, no. 10, pp. 3797–3800, Oct. 2008.
[5] H. J. Richter, A. Y. Dobin, O. Heinonen, K. Z. Gao, R. J. M. V. D. Veerdonk, R. T. Lynch, J. Xue, D. Weller, P. Asselin, M. F. Erden, and R. M. Brockie, "Recording on bit-patterned media at densities of 1 Tb/in^2 and beyond," *IEEE Trans. Magn.*, vol. 42, no. 6, pp. 2255–2260, Jun. 2006.
[6] B. D. Belle, F. Schedin, T. V. Ashworth, P. W. Nutter, E. W. Hill, H. J. Hug, and J. J. Miles, "Temperature dependence remanence loops of ion-milled bit patterned media," *IEEE Trans. Magn.*, vol. 44, no. 10, pp. 3468–3471, Oct. 2008.
[7] S. Nabavi, B. V. K. Vijaya Kumar, and J. A. Bain, "Two-dimensional pulse response and media noise modeling for bit-patterned media," *IEEE Trans. Magn.*, vol. 44, no. 10, pp. 3789–3792, Oct. 2008.
[8] P. W. Nutter, D. McA. McKirdy, B. K. Middleton, D. T. Wilton, and H. A. Shute, "Effect of island geometry on the replay signal in patterned media storage," *IEEE Trans. Magn.*, vol. 40, no. 10, pp. 3551–3557, Oct. 2004.
[9] P. W. Nutter, I. T. Ntokas, and B. K. Middleton, "An investigation of the effects of media characteristics on read channel performance for patterned media storage," *IEEE Trans. Magn.*, vol. 41, no. 11, pp. 4327–4334, Nov. 2005.
[10] S. Jeon and B. V. K. Vijaya Kumar, "Error event analysis of partial response targets for perpendicular magnetic recording," in *Proc. IEEE Global Telecommun. Conf.*, 2007, pp. 277–282.